Translational Oncology 50 (2024) 102136

Contents lists available at ScienceDirect

Translational Oncology

journal homepage: www.elsevier.com/locate/tranon

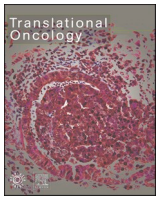

Original Research

Dronedarone hydrochloride inhibits gastric cancer proliferation *in vitro* and *in vivo* by targeting SRC

Xuebo Lu [a,b,1], Weizhe Zhang [a,b,1], Xiaoxiao Yang [a,b], Xiao Yan [a], Zubair Hussain [a], Qiong Wu [a,b], Jinmin Zhao [a], Baoyin Yuan [a], Ke Yao [b], Zigang Dong [a,b,c,d,f], Kangdong Liu [a,b,c,d,e,f], Yanan Jiang [a,b,c,d,e,f,*]

[a] *The Pathophysiology Department, The School of Basic Medical Sciences, Zhengzhou University, Zhengzhou 450000, China*
[b] *Tianjian Laboratory of Advanced Biomedical Sciences, Zhengzhou 450000 Henan, China*
[c] *China-US (Henan) Hormel Cancer Institute, Zhengzhou 450000, China*
[d] *State Key Laboratory of Esophageal Cancer Prevention and Treatment, Zhengzhou 450000, Henan, China*
[e] *Provincial Cooperative Innovation Center for Cancer Chemoprevention, Zhengzhou University 450000, Zhengzhou, Henan, China*
[f] *Cancer Chemoprevention International Collaboration Laboratory, Zhengzhou 450000, Henan, China*

ARTICLE INFO

Keywords:
Gastric cancer
Dronedarone hydrochloride
Cell proliferation
SRC/AKT1 signaling pathway

ABSTRACT

Background: Gastric cancer (GC) is a significant global concern, ranking as the fifth most prevalent cancer. Unfortunately, the five-year survival rate is less than 30 %. Additionally, approximately 50 % of patients experience a recurrence or metastasis. As a result, finding new drugs to prevent relapse is of utmost importance.
Methods: The inhibitory effect of Dronedarone hydrochloride (DH) on gastric cancer cells was examined using proliferation assays and anchorage-dependent assays. The binding of DH with SRC was detected by molecular docking, pull-down assays, and cellular thermal shift assays (CETSA). DH's inhibition of Src kinase activity was confirmed through *in vitro* kinase assays. The SRC knockout cells, established using the CRISPR-Cas9 system, were used to verify Src's role in GC cell proliferation. Patient-derived xenograft (PDX) models were employed to elucidate that DH suppressed tumor growth *in vivo*.
Results: Our research discovered DH inhibited GC cell proliferation *in vitro* and *in vivo*. DH bound to the SRC protein to inhibit the SRC/AKT1 signaling pathway in gastric cancer. Additionally, we observed a decrease in the sensitivity of gastric cancer cells to DH upon down-regulation of SRC. Notably, we demonstrated DH's anti-tumor effects were similar to those of Dasatinib, a well-known SRC inhibitor, in GC patient-derived xenograft models.
Conclusion: Our research has revealed that Dronedarone hydrochloride, an FDA-approved drug, is an SRC inhibitor that can suppress the growth of GC cells by blocking the SRC/AKT1 signaling pathway. It provides a scientific basis for use in the clinical treatment of GC.

Introduction

Gastric cancer (GC) is the fifth most prevalent cancer, with over one million confirmed cases and approximately 660,175 estimated deaths in 2022 [1]. Systemic treatment for gastric cancer has made significant advances in recent years, including targeted therapies, immunotherapy, optimization of radiotherapy and chemotherapy, and personalized treatment approaches [2-5]. Trastuzumab, a drug targeting HER2, has demonstrated effectiveness in treating gastric cancer. Unfortunately, only 22.1 % of gastric cancer cases are HER2-positive, and over 50 % of HER2-positive patients still do not respond to trastuzumab. Moreover, most patients develop resistance to trastuzumab within a year [6,7]. Due to reasons, such as drug resistance, side effects, and individual differences, the five-year survival rate for advanced gastric cancer is less than 40 %, with over 50 % of patients experiencing recurrence or metastasis after radical resection [8,9]. Hence, there is an urgent need to identify new molecular targets and drugs to improve the prognosis of GC patients.

Drug repurposing offers a approach to the drawbacks of high costs and lengthy development times associated with traditional drug

* Corresponding author at: Department of Pathophysiology, School of Basic Medical Sciences, Zhengzhou University, Zhengzhou, Henan 450000, China.
E-mail address: yananjiang@zzu.edu.cn (Y. Jiang).
[1] These authors contributed equally to this work.

https://doi.org/10.1016/j.tranon.2024.102136
Received 3 May 2024; Received in revised form 11 September 2024; Accepted 19 September 2024

development processes [10,11]. One practical and safe strategy for drug development involves screening FDA-approved drug libraries for potential cancer chemo-preventive agents. Through drug repurposing strategies, it is possible to identify new drugs to reduce clinical drug side effects, expand the clinical indications of drugs, and overcome resistance to radiotherapy and chemotherapy [12-14]. Recently, our research group discovered that oxethazaine [15] and tegaserod maleate [16] have anti-tumor effects in esophageal squamous cell carcinoma. These findings provide a rationale for using FDA-approved drugs in cancer chemoprevention.

The aberrant activation of SRC plays a significant role in regulating cell proliferation, adhesion, invasion, migration, and angiogenesis during tumor progression [17-19]. Moreover, SRC participates in multiple processes of tumorigenesis and development by phosphorylating AKT1 [20]. Studies have shown that inhibiting the SRC/AKT1 pathway can suppress cancer cell proliferation, invasion, and migration while promoting apoptosis [21,22].

In our study, we have demonstrated that Dronedarone hydrochloride (DH) can inhibit the growth of gastric cancer. Mechanistically, DH binds with SRC and inhibits its kinase activity, thereby suppressing the downstream pathway and inhibiting the proliferation of gastric cancer cells. These findings strongly provide a potential rationale for using DH in the chemoprevention of gastric cancer.

Materials and methods

Cell culture

The HGC27 and AGS cell lines were bought from the Chinese Academy of Sciences Cell Bank (Shanghai, China). The cells were verified to be mycoplasma-free and authenticated by STR analysis. HGC27 cells (cultured in RPMI 1640 medium containing 10 % fetal bovine serum) and AGS cells (cultured in F12K medium containing 10 % fetal bovine serum) were incubated at 37 °C with 5 % CO_2.

Cytotoxicity assay

The HGC27 and AGS (8000 cells/well) were seeded in 96-well plates and incubated with various concentrations of DH (0, 3.125, 6.25, 12.5, 25, 50 μM) for 24 and 48 h. After treatment, the cells were fixed and stained with DAPI at a dilution of 1:10000, and subsequently, cell counts were performed using IN Cell Analyzer 6000.

Proliferation assay

In this assay, HGC27 and AGS cells (3000 cells/well) were seeded into 96-well plates and incubated with various concentrations of DH (0, 0.5, 1, 2, and 4 μM) at different times (0, 24, 48, 72, and 96 h). After incubation, 10 μL MTT (5 mg/mL) was added to each well, and the cells were incubated at 37°C for 2 h. Next, 100 μL DMSO was added to each well, and the OD value was measured at 490 nm.

Anchorage-dependent assay

We seeded 400 HGC27 and AGS cells into each well of 6-well plates and treated them with DH at concentrations of 0, 0.5, 1, 2, and 4 μM. After incubating for 14 days, the colonies were stained with crystal violet and counted after photographing.

Anchorage-independent assay

HGC27 and AGS cells (8000 cells/well) were seeded onto the top gel containing 10 % FBS and 0.3 % agar with DH at 0, 0.5, 1, 2, and 4 μM. After a 7-day incubation, the colonies were photographed and analyzed using IN Cell Analyzer 6000 software.

Molecular docking assay

The crystal structure of SRC (PBD ID: 1YOM) was downloaded from the PDB database (www. rcsb.org/pdb), while the structural formula for DH was obtained from the PubChem database (https://pubchem.ncbi.nlm.nih.gov/). The docking analysis was performed using the AutoDock 4.2.6 software, and the resulting optimal complex was visualized by PyMOL (version 2.3.4).

Western blot assay

The cells were treated with DH at 0, 0.5, 1, 2, and 4 μM, and incubated for 24 h. The cells were collected, and their protein concentration was quantified using the BCA reagent. Then, SDS-PAGE gels were used to separate the protein, and the PVDF membrane was used to transfer the isolated protein for 2 h at 90V. After incubating with 1 % fat-free milk for 2 hours, the membrane was incubated with the primary antibody overnight at 4°C. Finally, bands were incubated with the corresponding secondary antibodies and visualized using the Tanon 5200.

Pull down assay

The DH-conjugated sepharose 4B beads or sepharose 4B beads alone were incubated with SRC protein or cell lysates in reaction buffer (2 mg/mL BSA, 50 mM Tris-HCl pH7.4, 200 mM NaCl, 5 mM EDTA, 1 mM dithiothreitol, and 0.01 % NP40) at 4 °C for 24 hours. The beads were washed thrice with the washing buffer, adding 30 μL loading buffer and heating at 95 °C for 5 mins. Finally, the binding was assessed by Western blot.

Cellular thermal shift assay (CETSA)

Cells were cultured in 15-cm dishes treated with DH (0 or 8 μM) for 3 h, then harvested and resuspended in PBS. Then, they were divided equally into 12 tubes. The control group and DH treatment group were heated at 37°C, 40°C, 43°C, 46°C, 49°C, 52°C, 55°C, 58°C, 61°C, 64°C, 67°C, and 70°C for 3 min. The samples were then quickly frozen twice in liquid nitrogen and centrifuged at 12000 rpm for 20 min at 4°C. The protein pellets were transferred to new tubes and kept on ice for 30 min before being finally analyzed by Western blot.

In vitro kinase assay

The active SRC (1000 ng) kinases were blended with different concentrations of DH (0, 0.5, 1, 2, and 4 μM) in kinase buffer II (Cat#K02–09, SignalChem, Canada). The inactive AKT1 proteins (100 ng), 100 μM adenosine triphosphate (ATP), and kinase buffer II were added and incubated for 30 min at 30°C. The reactions were terminated by loading buffer and heated for 5 min at 95°C, followed by the detection of SRC activity using an anti-p-AKT1 S473 antibody.

Tissue array

The tissue array (HStmA180Su09) comprised tumors and adjacent tissues from 78 gastric cancer cases was purchased from Outdo Biotech Company (Shanghai, China). SRC proteins were detected according to standard immunohistochemical methods, and their protein levels were evaluated and scored based on staining intensity and area. The tissue array was photographed and analyzed by Tissue Faxs (TissueGnostics, version 4.2).

Cell immunofluorescence assay

The GC cells were seeded on the slides, which were placed in a 24-well plate for 18 h and then treated with DH (0, 0.5, 1, 2, 4 μM) for 24 h. After discarding the medium, the cells were fixed with 4 %

Table 1
The oligonucleotide sequences of SRC single guide (sg) RNA primers of SRC

Gene Name	Primer sequences 5′-3′
SRC#2	F: CACCGCCGAGCCCAAGCTGTTCGG R: AAACCCGAACAGCTTGGGCTCGGC
SRC#5	F:CACCGACCTGGAACGGTACCACCA R: AAACTGGTGGTACCGTTCCAGGTC

Table 2
Information of human gastric cancer-derived xenograft tumor cases

Cancer type	Cancer number	Gender	Age	T	N	M	Pathological grading
Gastric cancer	LSG164	Male	75	3	1	0	IIb
Gastric cancer	LSG85	Female	65	4a	0	0	IVa
Gastric cancer	HSG288	Male	67	4a	2	0	IVa

paraformaldehyde. The slides with cells were incubated with the primary antibody for 12 h at 4°C, followed by incubation with the fluorescent secondary antibody for 2 h in the dark box. The slides were washed and stained with DAPI (1:10000) for 5 min at 37°C. The images were captured and analyzed using the IN Cell Analyzer 6000.

CRISPR/Cas 9 knockout cell lines

The GC cells were knocked out of the Src gene by the CRISPR/Cas9 system. The oligonucleotide sequences of SRC single guide (sg) RNA were designed using an online CRISPR tool (https://chopchop.cbu.uib.no/) and were listed in Table 1. The sgSRC plasmids were transfected into HEK293T cells by Jet Primer (Thermo Fisher Scientific, Waltham, MA, USA) following standard protocols. After 2 days, viral particles were harvested and filtered using a 0.22 μm filter. The GC cells were infected with 8 μg/mL polybrene and selected with 2 mg/mL puromycin for 72 h. The knockout efficiency was verified by Western blot.

PDX models

According to the guidelines of the Ethics Committee of Zhengzhou University (Zhengzhou, Henan, China), 5-8 weeks old female severe combined immunodeficiency (SCID) female mice (Cyagen Biosciences, China) were used to establish PDX models. The PDX models were established and obtained from three gastric cancer cases (LSG164, LSG85, and HSG288) (Table 2). Once the average tumor volume reached 100 mm^3, the mice were randomly divided into 3 or 4 groups: (1) the vehicle group, the low-dose DH group (30mg/kg), the high-DH dose group (120mg/kg), or the Dasatinib group. Tumor volumes were calculated using the formula: tumor volume (mm^3) = (length × $width^2$)/2. The tumor tissues were excised when the volume reached approximately 1000 mm^3.

Immunohistochemistry (IHC)

The tumor tissues were embedded in paraffin and cut into 4 μm sections. The tissues were processed for antigen retrieval after being dewaxed and dehydrated. The tissue array or slides were dropped onto 3 % H_2O_2 for 8 min. The primary antibody was added and incubated at 4°C for 12 h, followed by incubation with the secondary antibody at 37°C for 20 min. Then, the slides or tissue array was stained with diaminobenzidine (DAB) for 2 min and counterstained with hematoxylin. Finally, the Tissue Faxs (TissueGnostics, version 4.2) was used to scan the slides or tissue array, and the Image Pro Plus software program (Media Cybernetics, Rockville, MD) was used to quantify the positive cell rates.

Statistical analysis

All quantitative results were expressed as mean ± SD. Statistical analyses were performed using SPSS 21 software (IBM, USA). Unless otherwise stated, they were analyzed by homogeneity of variance and one-way analysis of variance (ANOVA). Statistical significance was set at $p < 0.05$.

Results

Dronedarone hydrochloride inhibited GC cell proliferation in vitro

To verify the DH's anti-tumor effect on GC cells, we treated HGC27 and AGS cells with various concentrations of DH (0, 3.125, 6.25, 12.5, 25, and 50 μM). The half-inhibitory concentrations (IC50) of HGC27 and AGS cells were 9.504 and 8.739 μM at 24 h and 6.587 and 4.188 μM at 48 h, respectively (Fig. 1 B, C). To explore the effects of DH on gastric cancer cell proliferation, we treated HGC27 and AGS cells with DH (concentrations: 0, 0.5, 1, 2, and 4 μM). After 96 h of treatment, the inhibition ratios of HGC27 and AGS at 4 μM were 60.2 % and 88.4 %, respectively (Fig. 1 D, E). The anchorage-dependent and anchorage-independent cell growth assay was employed to evaluate the effect of DH. The colony formation inhibition rates of HGC27 and AGS were 89.21 % and 74.42 %, respectively, at 4 μM using the anchorage-dependent assay (Fig. 1 F). In line with the findings of the anchorage-dependent assay, DH inhibited the colony formation of GC cells (Fig. 1 G). Hence, the results suggest that DH inhibits the viability of GC cells *in vitro*.

Dronedarone hydrochloride bound directly to SRC kinase

We screened for proteins that may bind to DH using the AutoDock 4.2.6 software since DH had an inhibitory effect on the viability of GC cells. The results indicated that DH was associated with the SRC protein at residues LEU 276, ASP 351, and MET 344 (Fig. 2 A). To confirm the binding between DH and SRC, we conducted pull-down assays and verified that DH could bind with the recombinant SRC protein (Fig. 2 B). Next, we overexpressed SRC in HEK293F cells and found that DH could bind with SRC protein extracted from HEK293F cells (Fig. 2 C). Furthermore, we confirmed the binding of DH with endogenous SRC obtained from HGC27 and AGS cell lysate by pull-down assays (Fig. 2 D, Fig. 2 E). To assess the binding efficiency between protein and drugs in cells, we performed the CETSA. The results of CETSA illustrated that the melting temperature (Tm) values of HGC27 and AGS cells in the control group were 52.6 and 52.8 °C, respectively. In contrast, the Tm values of HGC27 and AGS cells in the DH treatment group were 65.2 and 60.2°C, respectively. The results indicated that the SRC protein was rapidly denatured and precipitated at high temperatures, whereas the GC cells treated with DH were more stable (Fig. 2 F, G, Fig.S1A, B). Overall, the results suggest that DH directly binds with SRC kinase.

SRC was highly expressed in GC and negatively correlated with the prognosis of GC patients

To evaluate the protein levels of SRC and its clinical correlation in GC, we stained SRC protein in tissue array by IHC (Fig. 3 A). We found that SRC protein levels were highly expressed in tumor tissues compared to adjacent tissues (Fig. 3 B, C). Further analysis indicated no significant correlation between SRC protein expression levels and TNM staging ($p = 0.358$), age ($p = 0.307$), gender ($p = 0.599$), tumor size ($p = 0.969$), or pathological grade ($p = 0.358$) (Table 3). To assess the correlation between SRC expression and gastric cancer, we analyzed data from the TCGA database and found that SRC transcript levels were higher in GC than in normal tissues (Fig. 3 D). Subsequently, Kaplan-Meier analysis also showed that overexpression of SRC was inversely correlated with the prognosis of patients with GC (Fig. 3 E). In conclusion, these findings

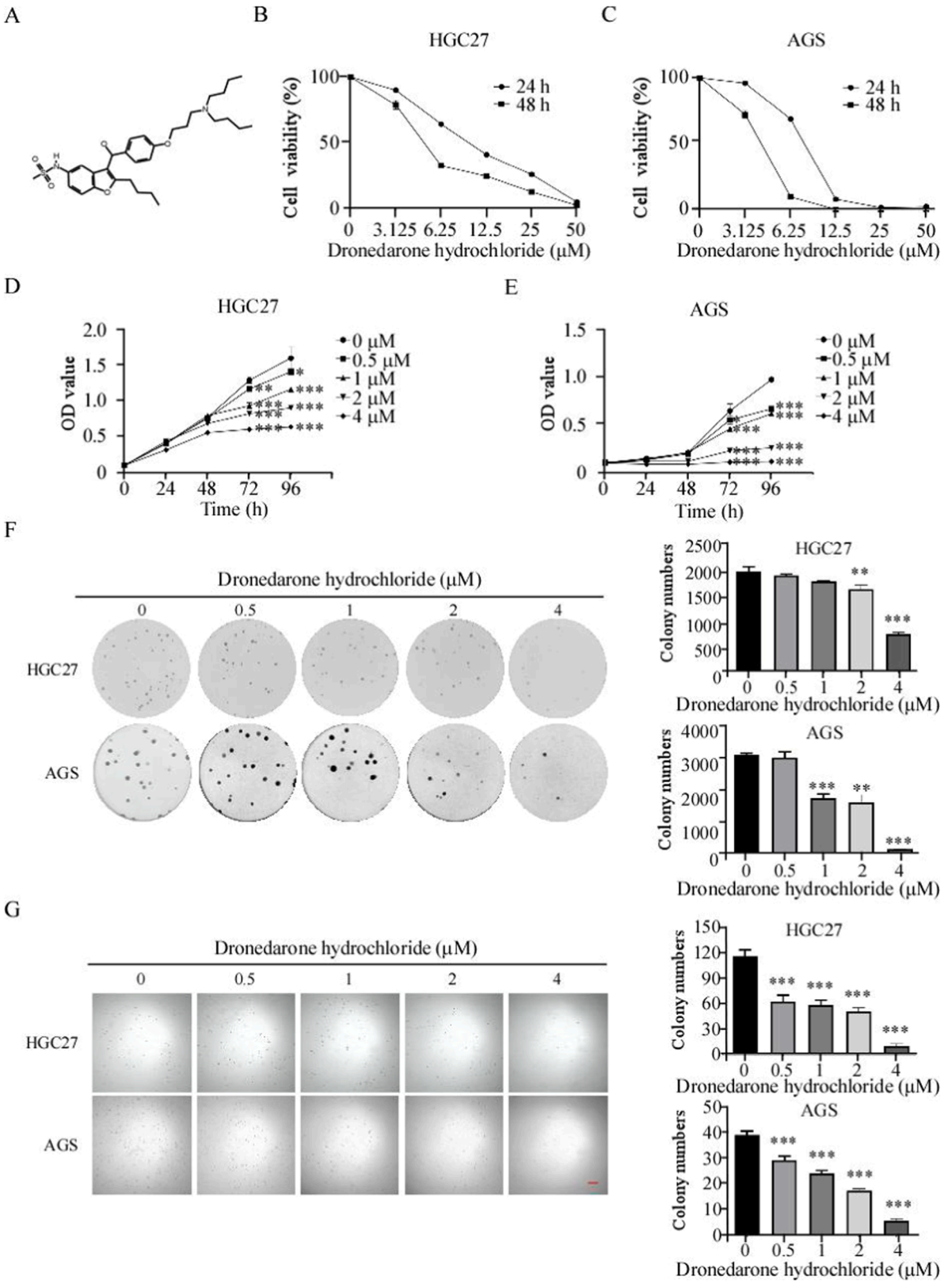

Fig 1. Dronedarone hydrochloride inhibited GC cell proliferation *in vitro*
(A) Chemical structure of Dronedarone hydrochloride. (B, C) The HGC27 (B) and AGS (C) cells were treated with DH at 0, 3.125, 6.25, 12.5, 25, and 50 μM for 24 and 48 h. The IC50 value of DH on gastric cancer cells. (D, E) The HGC27 (D) and AGS (E) cells were treated with DH for 24, 48, 72, and 96 h. The optical density (OD) value was evaluated by MTT assays and normalized to that of the control. (F) Gastric cancer cells were treated with various concentrations of DH (0, 0.5, 1, 2, and 4 μM) and measured at 7 days. (G) Gastric cancer cells were treated with various concentrations of DH (0, 0.5, 1, 2, and 4 μM) for 14 days, followed by crystal violet staining to monitor colony formation. Bar:50 μm. $^{*}p < 0.05$, $^{**}p < 0.01$, $^{***}p < 0.001$.

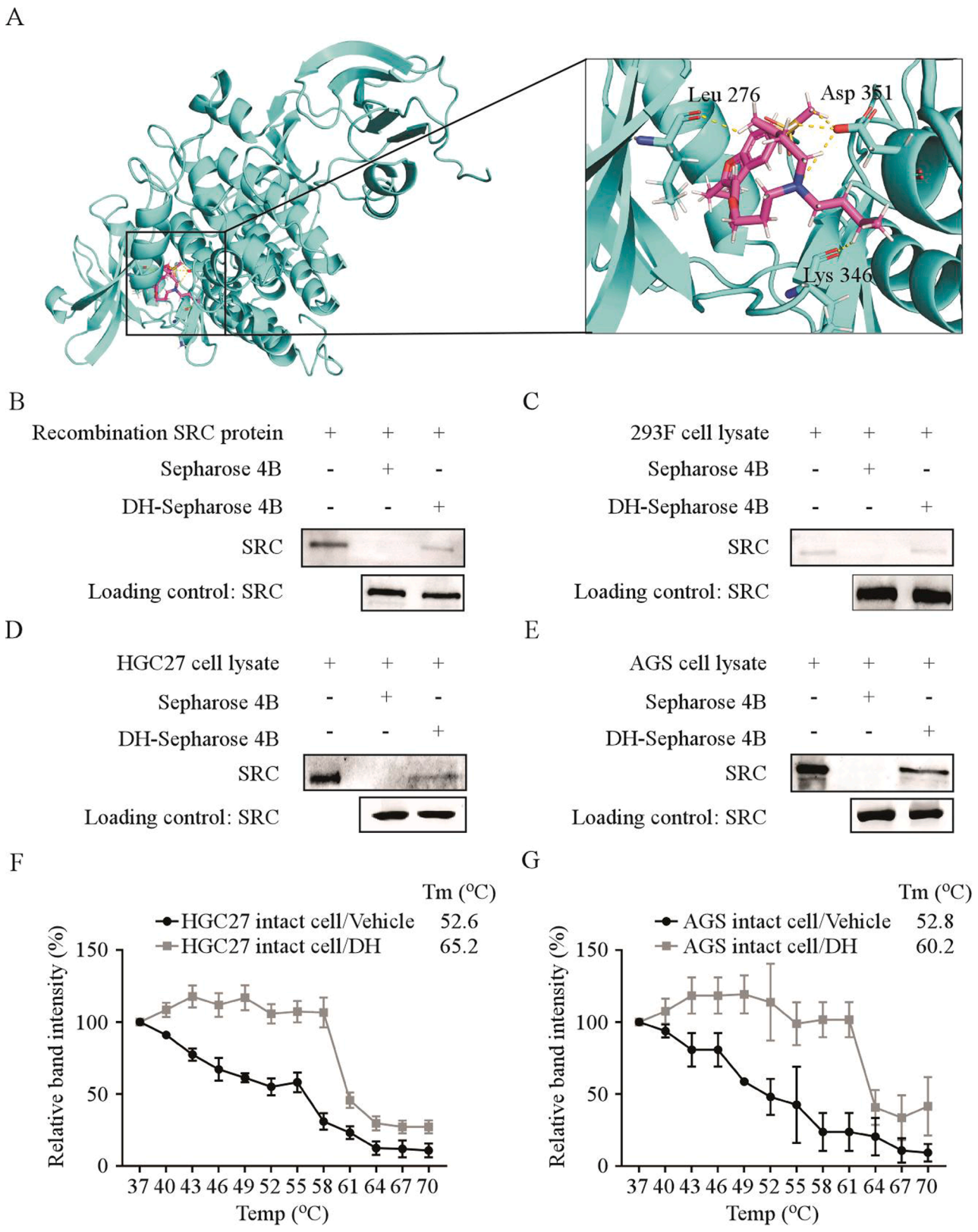

Fig 2. Dronedarone hydrochloride bound directly to SRC kinase
(A) Computational docking model between DH and SRC. (B–E) DH directly binds to SRC. The recombinant proteins (B) or cell lysates of HEK293F (C), HGC27 (D), and AGS (E) cells were incubated with DH-conjugated Sepharose 4B beads or with Sepharose 4B beads alone. The results were analyzed by Western blot. (F, G) The binding capacity of DH to SRC in gastric cancer intact cells. The HGC27 (F) and AGS (G) cells were treated with DH or DMSO for 24 h and at different temperatures. The protein bindings were visualized by Western blot.

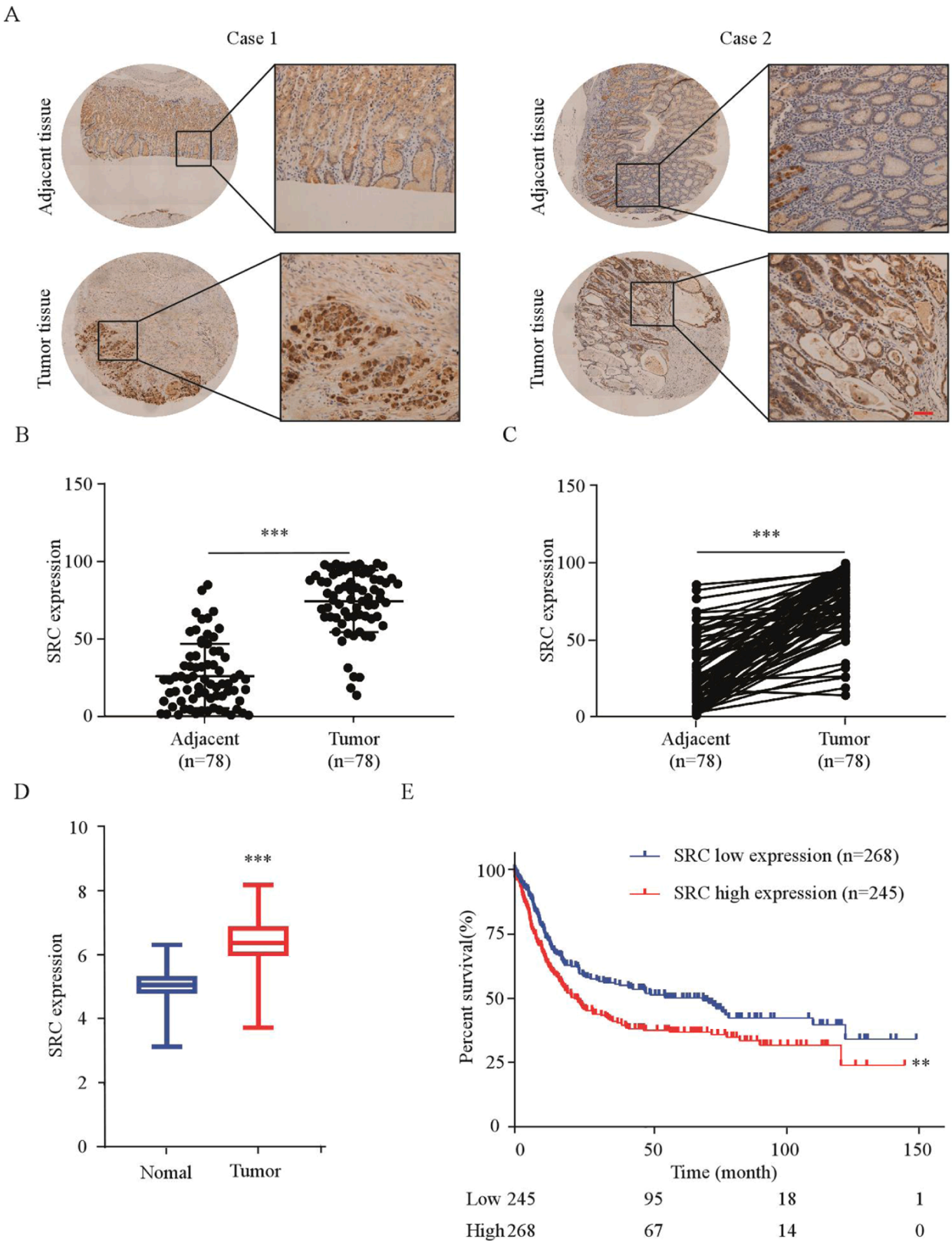

Fig. 3. SRC was highly expressed in GC and negatively correlated with the prognosis of GC patients
(A) Representative IHC staining images of human GC tissues detected using an SRC antibody. Scale bars: 50 μm. (B, C) Statistical analysis performed for IHC staining in unpaired (B) and paired (C) ESCC tissues; SRC expression is denoted as the positive percentage. (D) Distribution of SRC mRNA expression in normal tissues and gastric cancer tissues from Kaplan-Meier plotter (https://kmplot.com/analysis/). (E) Relationship between SRC expression levels and overall survival using the data from the TCGA database. *$p < 0.05$, **$p < 0.01$, ***$p < 0.001$

Table 3
Cohort characteristics of gastric cancer patients.

	SRC Expression		
	Low(n=42)	High(n=34)	*p* value
Gender			
Male	28(71.79 %)	30(78.95 %)	0.599
Female	11(28.21 %)	8(21.05 %)	
Age			
≤60	13(33.33 %)	8(20.51 %)	0.307
>60	26(66.67 %)	31(79.49 %)	
Tumor size			
≤5cm	4(10.26 %)	4(10.53 %)	0.969
>5cm	35(89.74 %)	34(89.47 %)	
pT status			
Tl+T2	4(11.76 %)	10(32.26 %)	0.117
T3	22(64.71 %)	14(45.16 %)	
T4	8(23.53 %)	7(22.58 %)	
PN status			
NO	11(28.21 %)	8(21.05 %)	0.456
Nl	4(10.26 %)	8(21.05 %)	
N2	9(23.08 %)	11(28.95 %)	
N3	15(38.36 %)	11(28.95 %)	
Clinical stage			
I	1(2.56 %)	4(10.26 %)	0.358
II	19(48.72 %)	16(41.03 %)	
III	19(48.72 %)	19(48.72 %)	

All data are the number of patients
Number do not equal to the total number due to missing data

indicate that SRC is highly expressed in gastric cancer and has a negative correlation with patient survival.

DH inhibited the SRC/AKT1 signaling pathway in gastric cancer

Prior studies have demonstrated that AKT1 can be activated by SRC kinase [23]. Therefore, we conducted an *in vitro* kinase assay using recombinant SRC protein to verify whether DH could inhibit SRC kinase activity. The results indicated that DH suppressed the phosphorylation of AKT1 *in vitro* (Fig. 4 A), indicating that DH suppressed AKT1 phosphorylation by inhibiting SRC kinase activity. Meanwhile, after 24 hours of receiving DH treatment, the Western blot results suggested that the reduction in AKT1 phosphorylation was directly proportional to the dosage. However, the total protein levels of AKT1 and SRC exhibited no noticeable changes (Fig. 4 B). Furthermore, we measured the phosphorylation levels of AKT1 by immunofluorescence assay. It was observed that the fluorescence intensity gradually decreased with the increase of the drug concentration (Fig. 4 C, D, Fig.S2A, B). Collectively, these findings indicated that DH suppressed the SRC/AKT1 pathways.

SRC knockout suppressed the sensitivity of gastric cancer cells to Dronedarone hydrochloride

To further investigate the role of SRC in gastric cancer growth, we established SRC knockout cell lines through the CRISPR/Cas9 system and verified the efficiency using Western blot. We confirmed that the protein levels of SRC and phosphorylation of AKT1 decreased in the sgSRC#2 and sgSRC#5 knockout cells (Fig. 5 A). Next, we assessed the effect of SRC knockout on GC cell proliferation by a cell proliferation assay and observed a decrease in GC cell proliferation after SRC

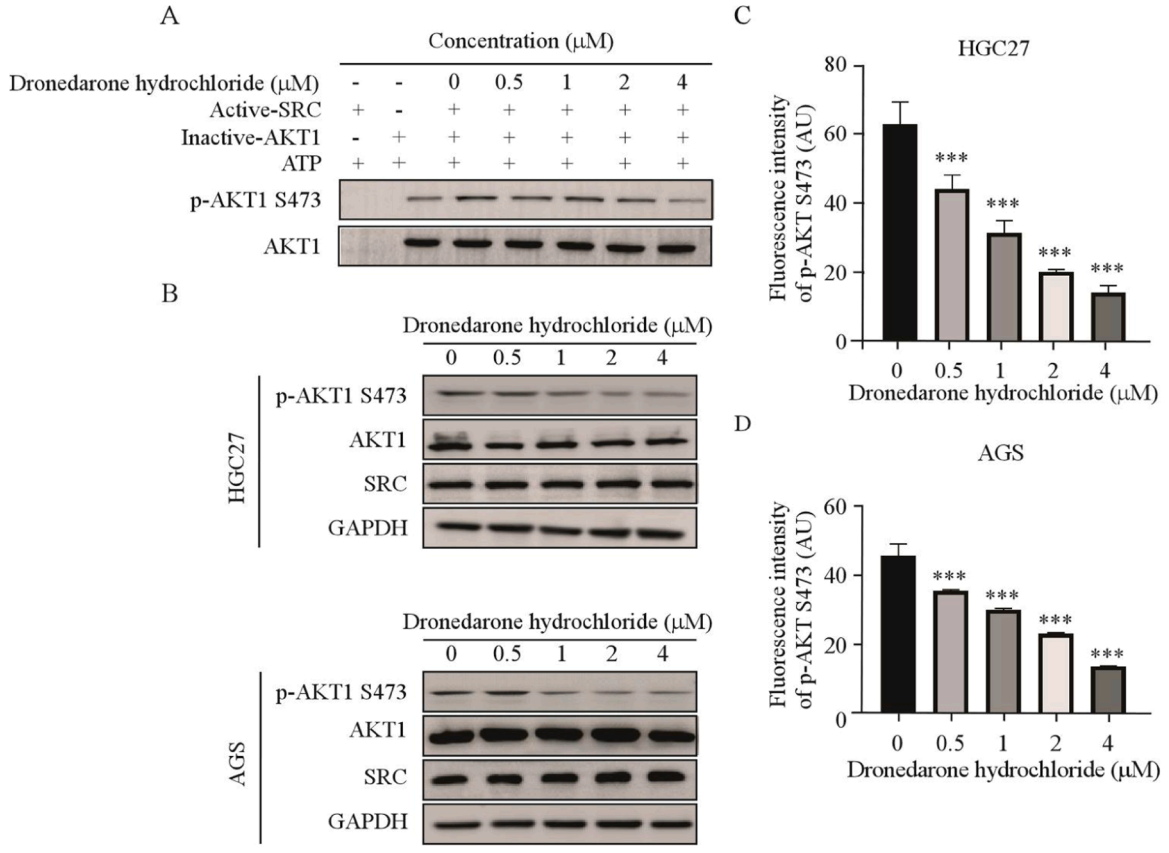

Fig. 4. DH inhibited the SRC/AKT1 signaling pathway in gastric cancer
(A) In vitro kinase assay of active SRC and inactive AKT1. The active SRC, inactive AKT1, and ATP mixture were treated with DH or DMSO at 30°C for 30 min, and p-AKT1 S473 was visualized by Western blot. (B) The levels of SRC/AKT1 signaling pathway in gastric cancer cells after DH (0, 0.5, 1, 2, and 4 μM) treatment. (C, D) Immunofluorescence staining of p-AKT1 S473 in the HGC27 (C) and AGS (D) cells after DH treatment. $^{*}p < 0.05$, $^{**}p < 0.01$, $^{***}p < 0.001$.

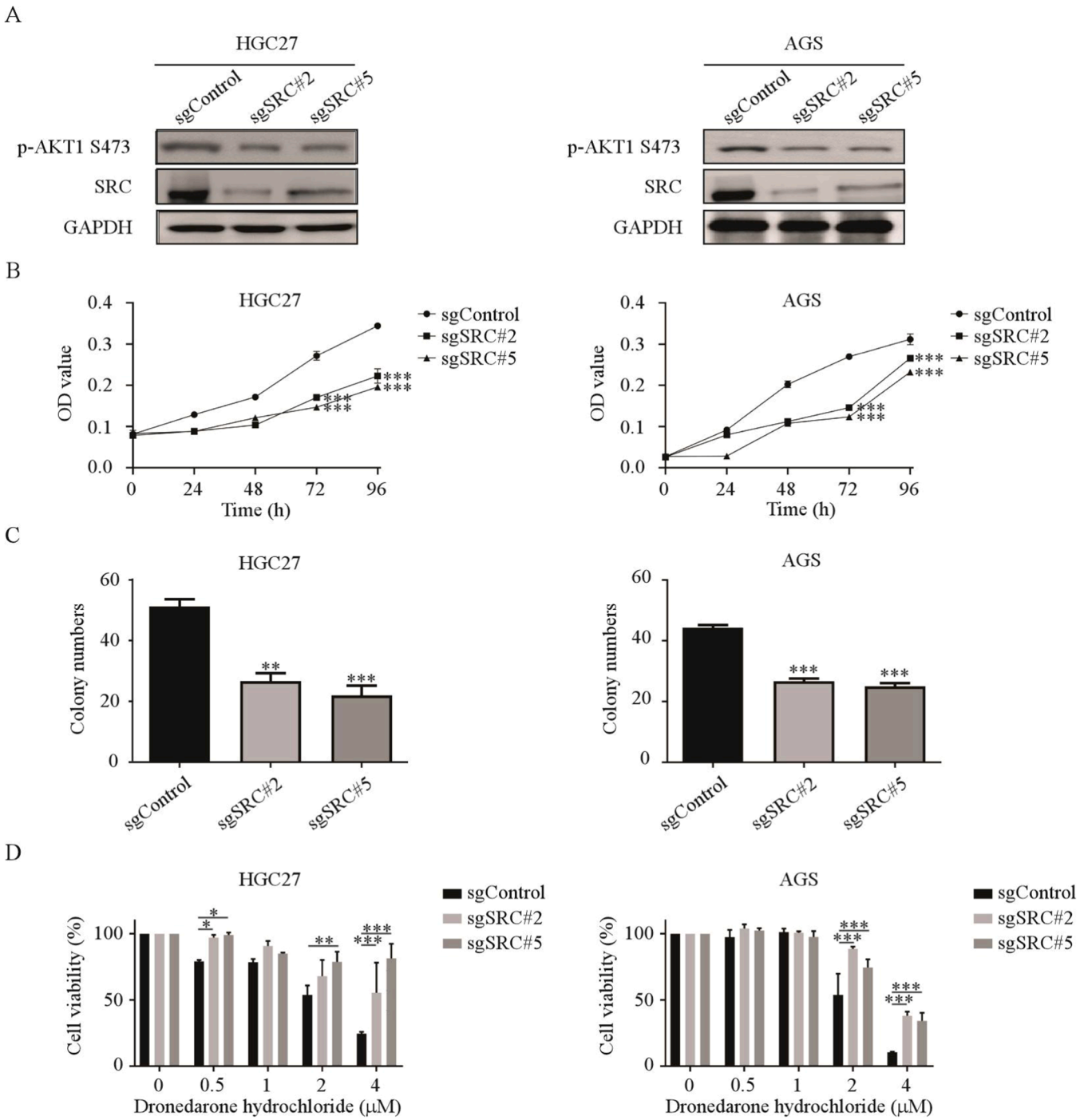

Fig. 5. SRC knockout suppressed the sensitivity of gastric cancer cells to Dronedarone hydrochloride
(A) The SRC and p-AKT1 protein expression in SRC knockout HGC27 and AGS cells by Western blot. (B) The cell viability in SRC knockout cells was evaluated by MTT assay and normalized to that of the control. (C) The colony-formation ability in SRC knockout cells was normalized to that of the control. (D) SRC knockout cells were treated with DH (0, 0.5, 1, 2, and 4 μM) for 96 h. The cell viability was evaluated by MTT assays and normalized to that of the sgControl cells. *$p < 0.05$, **$p < 0.01$, ***$p < 0.001$

knockout. Likewise, the colony formation ability of GC cells decreased after SRC knockout compared to the control group (Fig. 5 B, C, Fig. S3). To verify whether DH inhibits the proliferation of GC cells through SRC, we assessed the proliferation of sgSRC cells following the treatment of DH. We found that the cells in the control group decreased in a dose-dependent manner, while those in the SRC knockout group resisted DH treatment. This result indicated that the susceptibility of the SRC knockout cells to DH was significantly suppressed (Fig. 5 D). Thus, it can be inferred that SRC plays a critical effect in GC cell proliferation, and DH exerts its functions through SRC.

Dronedarone hydrochloride inhibited ESCC tumor growth in vivo

To investigate the anti-tumor effect of DH *in vivo*, we established two PDX models (LSG164 and LSG85). Briefly, the mice were administered either vehicle (0.9 % normal saline) or DH (30 mg/kg or 120 mg/kg) by oral gavage every day until the average tumor volume of the control group reached the endpoint (1000 mm^3). It was observed that the tumor

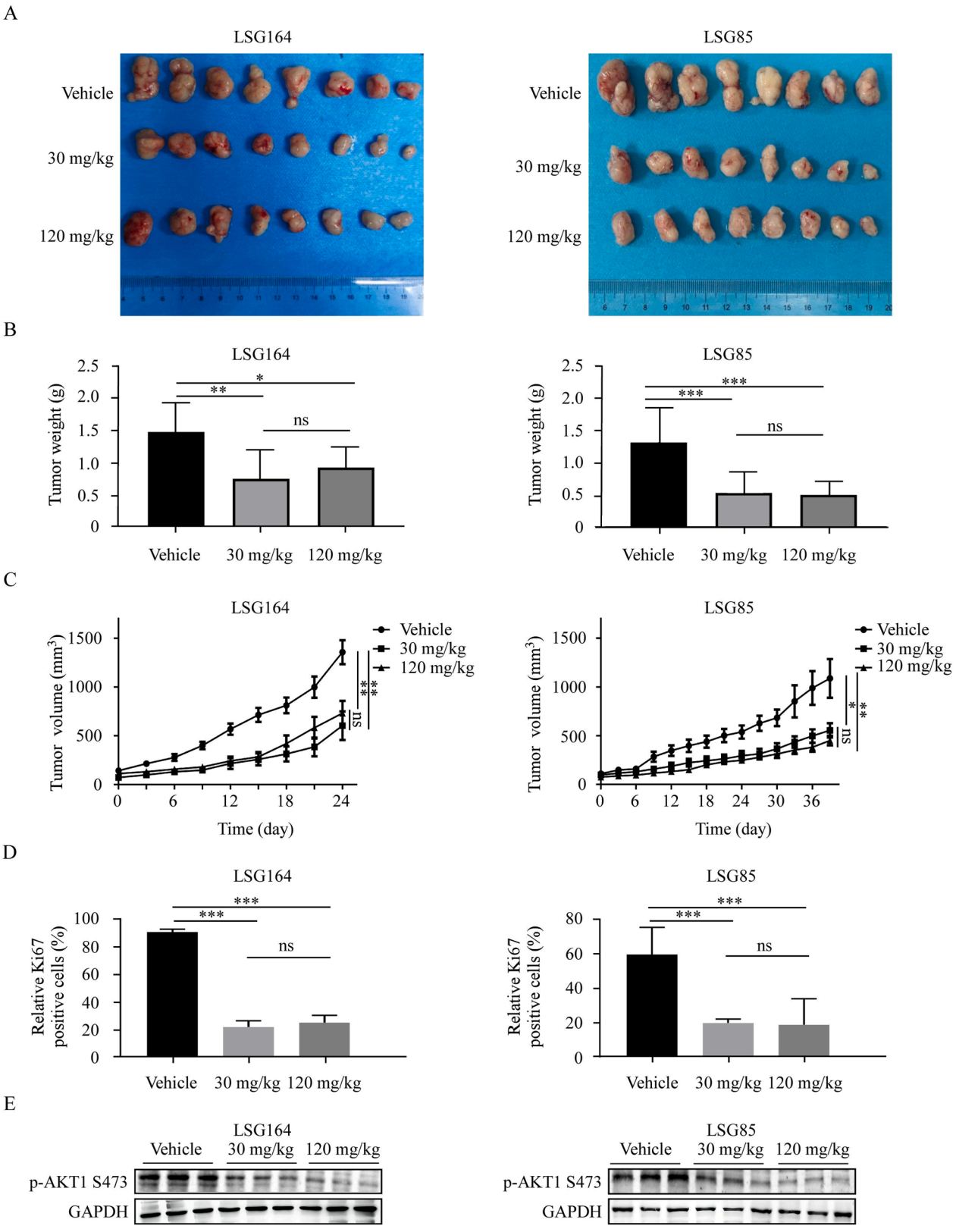

Fig. 6. Dronedarone hydrochloride inhibited tumor growth *in vivo*
(A) The SCID mice with LSG164 or LSG85 xenografts were treated by 30 and 120 mg/kg DH. Tumor images of xenografts in different groups after sacrificing. (B) The tumor weights of the Vehicle and DH groups were measured. (C) The tumor volumes of vehicle and DH groups were measured. (D) Immunohistochemistry was used to analyze the Ki67 levels in tumor tissues from treated or untreated groups of mice. (E) Western blot was used to analyze the p-AKT1 S473 levels in tumor tissues from treated or untreated groups of mice. *$p < 0.05$, **$p < 0.01$, ***$p < 0.001$.

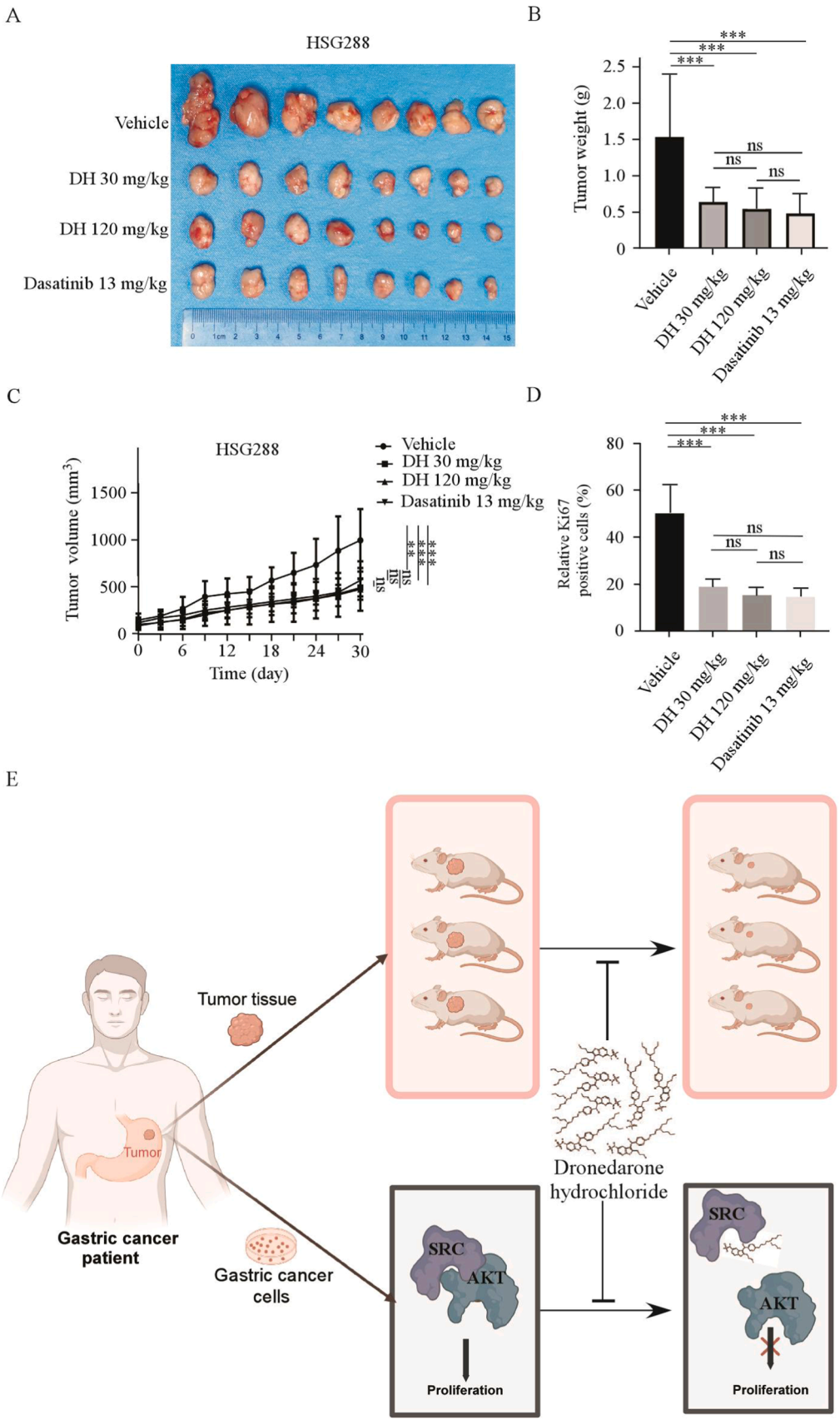

Fig. 7. Dronedarone hydrochloride exerted the same anti-tumor activities as Dasatinib *in vivo*
(A) Tumor images of HSG288 xenografts in the 30 and 120 mg/kg DH and 13 mg/kg Dasatinib group. (B) and (C) The tumor volumes and weights of Vehicle, DH, and Dasatinib groups were measured. (D) Immunohistochemistry was used to analyze the protein levels of Ki67 in tumor tissues from treated or untreated groups of mice. $^{*}p < 0.05$, $^{**}p < 0.01$, $^{***}p < 0.001$. (E) The schematic drawing shows that DH inhibits GC growth by inhibiting the SRC/AKT pathway *in vitro* and *in vivo*.

weights in the DH-treated group were significantly suppressed compared with the control group (Fig. 6 A, B). In addition, we observed a significant decrease in tumor volume in mice treated with DH compared to the control group (Fig. 6 C). Moreover, we performed Ki67 staining to assess the effect of DH on cell proliferation and found that the expression of Ki67 was reduced in the DH-treated group (Fig. 6 D, S4A). Furthermore, Western blot analysis showed that DH treatment led to suppression of AKT1 phosphorylation in the tumor tissues (Fig. 6 E). In short, these results demonstrate that DH inhibits the growth of GC *in vivo*.

Dronedarone hydrochloride exerted the same anti-tumor activities as Dasatinib in vivo

Dasatinib, an inhibitor of SRC tyrosine kinases, is currently used to treat chronic myeloid leukemia [24]. To compare the anti-tumor effects of DH and Dasatinib, we established a PDX model. Briefly, the mice were gavaged with vehicle (0.9 % normal saline), DH (30 mg/kg or 120 mg/kg), or Dasatinib (13 mg/kg) daily. Both DH and Dasatinib treatments significantly reduced tumor volume compared to the control group, and there was no significant difference in tumor volumes between the DH and Dasatinib treatment groups (Fig. 7 A, B). In addition, tumor weight was significantly reduced in the treated DH and Dasatinib groups compared to the control group. There was no significant difference in tumor weight between each treatment group (Fig. 7 C). Subsequently, IHC analysis of Ki-67 showed that proliferation decreased following treatment with DH and Dasatinib (Fig. 7 D, Fig. S4B). In conclusion, DH exerts the same anti-tumor activities as Dasatinib *in vivo*.

Discussion

Accumulating evidence indicates chemoprevention plays a critical role in cancer occurrence and recurrence [25-27]. Therefore, finding a drug to avoid GC occurrence and recurrence is essential to reduce the incidence and improve the prognosis of GC patients. As a drug development strategy, drug repositioning provides a safer and more effective treatment for the disease using existing drugs [28-30]. Through this strategy, we have found that DH significantly suppresses cell proliferation and clone formation of GC cells.

Signal transduction pathways play a critical role in the occurrence and progression of tumors [31]. For example, MAPK, PI3K/AKT, and Wnt/β-catenin pathways regulate cell proliferation, apoptosis, migration, invasion, and angiogenesis, thereby promoting tumor formation and development [32,33]. SRC plays a significant role in these signaling pathways [17,18,21]. Studies have shown that SRC is found to be over-activated in colon cancer, breast cancer, pancreatic cancer, and lung cancer [34,35]. Our study demonstrated that the mRNA level and protein level of SRC were highly expressed in GC and negatively correlated with the prognosis of GC patients. Furthermore, knocking out SRC suppressed the proliferation of GC cells. Therefore, targeting SRC may become an effective strategy for the treatment of gastric cancer.

In our study, we have demonstrated that Dronedarone hydrochloride targeted SRC and inhibited its activity. Moreover, the sensitivity of GC cells to DH was reduced by knocking out SRC. The SRC/AKT1 pathway mediates the proliferation, apoptosis, autophagy, and migration of tumor cells [36], and phosphorylated AKT1 can promote cell proliferation [37]. We inferred that DH inhibited the phosphorylation of AKT1 by inhibiting the kinase activity of SRC. Thus, DH treatment inhibited the SRC/AKT1 signaling pathway in GC cells and effectively suppressed the growth of GC. This study holds significant potential as it introduces DH as a promising candidate for GC treatment.

Previous studies have shown that some SRC inhibitors, such as Dasatinib [38], Saracatinib [39], and Bosutinib [40], have therapeutic effects in liver cancer, small-cell lung cancer, and chronic myelogenous leukemia. However, these SRC inhibitors have not been applied to treat GC in clinical. DH is an FDA-approved antiarrhythmic drug with established safety data. Notably, we discovered that DH significantly suppressed GC growth *in vivo*, suggesting the importance of conducting further clinical trials. Moreover, we found that DH exerted the same anti-tumor activities as Dasatinib *in vivo*. Studies have shown that some patients have severe cardiovascular injury [41] during treatment with Dasatinib. In addition, patients may also have adverse reactions, including bleeding, pleural effusion [42,43], pulmonary hypertension [44], liver injury [45] and renal failure [46]. In comparison, patients taking DH may experience only mild gastrointestinal adverse reactions, such as nausea, diarrhea, and vomiting [47-49]. This indicates that DH has a better safety profile compared to Dasatinib.

Our study highlights the potential of DH as a chemopreventive agent for GC. However, there are still some limitations that need to be addressed. Firstly, DH's efficacy and safety should be further confirmed in pre-clinical trials. Secondly, the effects of DH on other biological processes remain unclear, and further research is needed to explore its impact on these biological processes. Nevertheless, as DH is an FDA-approved drug with established safety data, repurposing it for gastric cancer treatment could accelerate the transition from bench to bedside.

In conclusion, our results suggest that DH effectively inhibits the growth of gastric cancer *in vitro* and *in vivo*. This study declares that the careful application of DH could serve as a promising chemopreventive approach for GC patients with high expression of SRC.

Ethics approval and consent to participate

All animal experiments in this study were conducted with the approval of the ethics committee of Zhengzhou University (ZZUIRB2022-71). All patients provided written informed consent for the use of the tissue samples.

Consent

This study does not involve clinical patients

CRediT authorship contribution statement

Xuebo Lu: Writing – original draft, Software, Data curation. **Weizhe Zhang:** Writing – original draft, Software, Data curation. **Xiaoxiao Yang:** Writing – original draft, Methodology, Data curation. **Xiao Yan:** Writing – review & editing, Data curation. **Zubair Hussain:** Software, Investigation. **Qiong Wu:** Supervision, Methodology, Formal analysis. **Jinmin Zhao:** Writing – review & editing, Supervision, Resources. **Baoyin Yuan:** Supervision, Resources. **Ke Yao:** Supervision, Resources, Methodology. **Zigang Dong:** Supervision, Resources, Formal analysis. **Kangdong Liu:** Writing – review & editing, Supervision, Funding acquisition, Formal analysis. **Yanan Jiang:** Writing – review & editing, Resources, Funding acquisition.

Declaration of competing interest

The authors have no relevant financial or nonfinancial interests to disclose

Data availability

There is no data availability.

Funding

This work was supported by the National Natural Science Foundation of China (82473228, 82472998), the Fundamental Research Project of Key Scientific Research in Henan Province (23ZX007), the Science and Technology Project of Henan Province (No. 242102311082), the Central Plains Science and Technology Innovation Leading Talents

(224200510015), National Natural Science Youth Foundation (81902486, 82303119). We thank all members of our team for their critical input and suggestions.

Supplementary materials

Supplementary material associated with this article can be found, in the online version, at doi:10.1016/j.tranon.2024.102136.

References

[1] J. Ferlay, et al., Global cancer observatory: cancer today, Lyon: International agency for research on cancer (2020). **20182020**.
[2] A. Rizzo, et al., Hypertransaminasemia in cancer patients receiving immunotherapy and immune-based combinations: the MOUSEION-05 study, Cancer Immunol Immunother 72 (6) (2023) 1381–1394.
[3] A. Rizzo, et al., Peripheral neuropathy and headache in cancer patients treated with immunotherapy and immuno-oncology combinations: the MOUSEION-02 study, Expert Opin Drug Metab Toxicol 17 (12) (2021) 1455–1466.
[4] F.G. Dall'Olio, et al., Immortal time bias in the association between toxicity and response for immune checkpoint inhibitors: a meta-analysis, Immunotherapy 13 (3) (2021) 257–270.
[5] D.C. Guven, et al., The association between albumin levels and survival in patients treated with immune checkpoint inhibitors: A systematic review and meta-analysis, Front Mol Biosci 9 (2022) 1039121.
[6] H.H. Hu, et al., HER2(+) advanced gastric cancer: Current state and opportunities (Review), Int J Oncol 64 (4) (2024).
[7] M. Moehler, et al., Recent progress and current challenges of immunotherapy in advanced/metastatic esophagogastric adenocarcinoma, Eur J Cancer 176 (2022) 13–29.
[8] C. Burz, et al., Prognosis and Treatment of Gastric Cancer: A 2024 Update, Cancers (Basel) 16 (9) (2024).
[9] D. Marrelli, et al., Prediction of recurrence after radical surgery for gastric cancer: a scoring system obtained from a prospective multicenter study, Annals of surgery 241 (2) (2005) 247–255.
[10] S. Pushpakom, et al., Drug repurposing: progress, challenges and recommendations, Nature reviews Drug discovery 18 (1) (2019) 41–58.
[11] V. Parvathaneni, et al., Drug repurposing: a promising tool to accelerate the drug discovery process, Drug Discov Today 24 (10) (2019) 2076–2085.
[12] Y. Qin, et al., Autophagy and cancer drug resistance in dialogue: Pre-clinical and clinical evidence, Cancer Lett 570 (2023) 216307.
[13] W. Zhang, et al., Cell membrane-camouflaged bufalin targets NOD2 and overcomes multidrug resistance in pancreatic cancer, Drug Resist Updat 71 (2023) 101005.
[14] M. Ashrafizadeh, et al., Molecular panorama of therapy resistance in prostate cancer: a pre-clinical and bioinformatics analysis for clinical translation, Cancer Metastasis Rev 43 (1) (2024) 229–260.
[15] Z. Bao, et al., Oxethazaine inhibits esophageal squamous cell carcinoma proliferation and metastasis by targeting aurora kinase A, Cell Death & Disease 13 (2) (2022) 189.
[16] X. Wu, et al., Tegaserod maleate inhibits esophageal squamous cell carcinoma proliferation by suppressing the peroxisome pathway, Frontiers in Oncology 11 (2021) 683241.
[17] S.M. Dehm, K. Bonham, SRC gene expression in human cancer: the role of transcriptional activation, Biochem Cell Biol 82 (2) (2004) 263–274.
[18] J.D. Bjorge, A. Pang, D.J. Fujita, Identification of protein-tyrosine phosphatase 1B as the major tyrosine phosphatase activity capable of dephosphorylating and activating c-Src in several human breast cancer cell lines, J Biol Chem 275 (52) (2000) 41439–41446.
[19] R.B. Irby, T.J. Yeatman, Role of Src expression and activation in human cancer, Oncogene 19 (49) (2000) 5636–5642.
[20] M.M. Rose, et al., AKT-independent signaling in PIK3CA-mutant thyroid cancer mediates resistance to dual SRC and MEK1/2 inhibition, Med Oncol 40 (10) (2023) 299.
[21] X. Luo, et al., The fatty acid receptor CD36 promotes HCC progression through activating Src/PI3K/AKT axis-dependent aerobic glycolysis, Cell Death Dis 12 (4) (2021) 328.
[22] N. Deng, X. Zhang, Y. Zhang, BAIAP2L1 accelerates breast cancer progression and chemoresistance by activating AKT signaling through binding with ribosomal protein L3, Cancer Sci 114 (3) (2023) 764–780.
[23] H.P. Zhang, et al., PI3K/AKT/mTOR signaling pathway: an important driver and therapeutic target in triple-negative breast cancer, Breast Cancer 31 (4) (2024) 539–551.
[24] Fauziya, et al., Dasatinib: a potential tyrosine kinase inhibitor to fight against multiple cancer malignancies, Med Oncol 40 (6) (2023) 173.
[25] N.F. Lange, P. Radu, J.F. Dufour, Prevention of NAFLD-associated HCC: Role of lifestyle and chemoprevention, J Hepatol 75 (5) (2021) 1217–1227.
[26] S. Patra, et al., Chemotherapeutic efficacy of curcumin and resveratrol against cancer: Chemoprevention, chemoprotection, drug synergism and clinical pharmacokinetics, Semin Cancer Biol 73 (2021) 310–320.
[27] M.B. Piazuelo, et al., The Colombian Chemoprevention Trial: 20-Year Follow-Up of a Cohort of Patients With Gastric Precancerous Lesions, Gastroenterology 160 (4) (2021) 1106–1117, e3.
[28] M.S. G, et al., Cancer Chemoprevention: A Strategic Approach Using Phytochemicals, Front Pharmacol 12 (2021) 809308.
[29] F. Napolitano, et al., Drug repositioning: a machine-learning approach through data integration, J Cheminform 5 (1) (2013) 30.
[30] E. Hernández-Lemus, M. Martínez-García, Pathway-Based Drug-Repurposing Schemes in Cancer: The Role of Translational Bioinformatics, Front Oncol 10 (2020) 605680.
[31] Z.N. Lei, et al., Signaling pathways and therapeutic interventions in gastric cancer, Signal Transduct Target Ther 7 (1) (2022) 358.
[32] D.T. Morgos, et al., Targeting PI3K/AKT/mTOR and MAPK Signaling Pathways in Gastric Cancer, Int J Mol Sci 25 (3) (2024).
[33] N. Krishnamurthy, R. Kurzrock, Targeting the Wnt/beta-catenin pathway in cancer: Update on effectors and inhibitors, Cancer Treat Rev 62 (2018) 50–60.
[34] X. Lu, et al., mPRα mediates P4/Org OD02-0 to improve the sensitivity of lung adenocarcinoma to EGFR-TKIs via the EGFR-SRC-ERK1/2 pathway, Mol Carcinog 59 (2) (2020) 179–192.
[35] A.R. Poh, M. Ernst, Functional roles of SRC signaling in pancreatic cancer: Recent insights provide novel therapeutic opportunities, Oncogene 42 (22) (2023) 1786–1801.
[36] S. Codenotti, et al., Statin-Sensitive Akt1/Src/Caveolin-1 Signaling Enhances Oxidative Stress Resistance in Rhabdomyosarcoma, Cancers (Basel) 16 (5) (2024).
[37] J. Jiang, et al., Quercetin inhibits breast cancer cell proliferation and survival by targeting Akt/mTOR/PTEN signaling pathway, Chem Biol Drug Des 103 (6) (2024) e14557.
[38] C. Liu, et al., Dasatinib inhibits proliferation of liver cancer cells, but activation of Akt/mTOR compromises Dasatinib as a cancer drug, Acta Biochimica et Biophysica Sinica 53 (7) (2021) 823–836.
[39] R. Ramos, N. Vale, Dual Drug Repurposing: The Example of Saracatinib, Int J Mol Sci 25 (8) (2024).
[40] F. Rusconi, et al., Bosutinib: a review of preclinical and clinical studies in chronic myelogenous leukemia, Expert Opin Pharmacother 15 (5) (2014) 701–710.
[41] Y. Liu, et al., YQFM Alleviates Side Effects Caused by Dasatinib through the ROCK/MLC Pathway in Mice, Evid Based Complement Alternat Med 2020 (2020) 4646029.
[42] J.E. Cortes, et al., Final 5-Year Study Results of DASISION: The Dasatinib Versus Imatinib Study in Treatment-Naïve Chronic Myeloid Leukemia Patients Trial, J Clin Oncol 34 (20) (2016) 2333–2340.
[43] T.P. Hughes, et al., Incidence, outcomes, and risk factors of pleural effusion in patients receiving Dasatinib therapy for Philadelphia chromosome-positive leukemia, Haematologica 104 (1) (2019) 93–101.
[44] C. Daccord, et al., First histopathological evidence of irreversible pulmonary vascular disease in Dasatinib-induced pulmonary arterial hypertension, Eur Respir J 51 (3) (2018).
[45] J.N. Justice, et al., Senolytics in idiopathic pulmonary fibrosis: Results from a first-in-human, open-label, pilot study, EBioMedicine 40 (2019) 554–563.
[46] R.C. Calizo, et al., Disruption of podocyte cytoskeletal biomechanics by Dasatinib leads to nephrotoxicity, Nat Commun 10 (1) (2019) 2061.
[47] P. Touboul, et al., Dronedarone for prevention of atrial fibrillation: a dose-ranging study, Eur Heart J 24 (16) (2003) 1481–1487.
[48] M. Kowalczyk, et al., Levosimendan - a calcium sensitising agent with potential anti-arrhythmic properties, Int J Clin Pract 64 (8) (2010) 1148–1154.
[49] D. Kozlowski, et al., Vernakalant hydrochloride for the treatment of atrial fibrillation, Expert Opin Investig Drugs 18 (12) (2009) 1929–1937.